Analysis of the ramp-down phase using the Fenix flight simulator

R. Coosemans[1], E. Fable[2], C. Contré[1], P. David[2], F. Felici[1], S. Medvedev[3], A. Merle[1], T. Pütterich[2], O. Sauter[1], S. Van Mulders[1], C. Wu[4], and the ASDEX Upgrade Team*

[1] *Ecole Polytechnique Fédérale de Lausanne (EPFL), Swiss Plasma Center (SPC), CH-1015 Lausanne, Switzerland*

[2] *Max-Planck-Institut für Plasmaphysik, 85748 Garching, Germany*

[3] *Tokamak Energy Ltd, Culham Science Centre, Abingdon, OX14 3DB, United Kingdom*

[4] *4 Karlsruher Institut für Technologie, 76344 Eggenstein-Leopoldshafen, Germany*

Introduction

The capability to accurately design plasma scenarios is crucial for the successful operation of future fusion reactors. However, the rich physics involved, the multitude of actuators available, and the trade-off between conflicting objectives and operating constraints make this a daunting task. So called "tokamak flight simulators" capable of simulating the complete discharge, including the interaction between the plasma and the control system, with reasonable accuracy in limited computational time provide a valuable tool to support this effort.

In this context, we use the Fenix flight simulator [1] to model ASDEX Upgrade (AUG) scenarios with varying ramp-down rates developed for the ITER baseline [2]. This complex ramp-down phase of the discharge will be critical in future reactors because of the high-energy plasma needing to be terminated in a safe and controlled way. Next to the interest of the underlying physics, this provides a challenging case for testing the Fenix flight simulator. In addition, we can exploit the synergy of these shots already having been modelled with the fast transport code RAPTOR in [3].

The Fenix flight simulator

The Fenix flight simulator has been developed to model complete discharges of AUG, i.e. including the ramp-up, flattop, and ramp-down phases. This code mainly integrates the ASTRA transport code [4] and the SPIDER free-boundary equilibrium code [5] in the PCSSP Simulink control framework [6]. Figure 1 shows a schematic of this coupling. Fenix simulates AUG discharges taking as only input the discharge program, as it is also fed to the AUG tokamak for experiments. This discharge program contains the reference trajectories for the various quantities of interest, which can include both references for the actuators (e.g. injected NBI power) or references for the plasma quantities to be achieved (e.g. target density). As output, Fenix provides the time trajectory of the state of the tokamak.

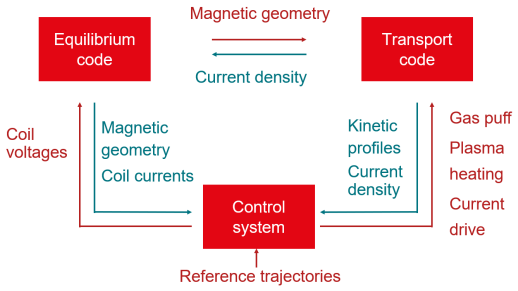

Figure 1: *Schematic of Fenix flight simulator*

The physics model used in Fenix is described in [1]. Table 1 summarises its main elements. It is expected that the empirical coefficients in the transport models indicated as non-generic in this table, and perhaps the corresponding models as a whole, will have to be adjusted for the

*See the author list of U. Stroth et al, 2022 Nucl. Fusion 62, 042006

application of Fenix to the TCV tokamak as is envisaged in future work. The control system will obviously also need to be replaced by that of TCV.

Table 1: Fenix model summary

			generic?
transport	ASTRA code [4]		
	NBI	Rabbit code [7]	yes
	ECRH	Torbeam code [8]	yes
	ICRH	gaussian distribution	yes
	radiation	Bremsstrahlung, synchrotron, impurities	yes
	current transport	neoclassical conductivity, bootstrap, sawtooth	yes
	heat transport	gyro-bohm-like in core region	no
		pedestal according to scaling law [9] in H-mode	no
		fixed edge diffusivity in L-mode pedestal	no
	particle transport	continuity equations for D,He,B,W,N,Ne,H,Kr,Ar	yes
		semi-empirical diffusion and convection coefficients	no
	SOL-divertor-wall	multi-zone model for particle content	no
		two-point model for separatrix temperatures [10]	yes
equilibrium	SPIDER free-boundary code [5]		yes
control system	PCSSP-Simulink [6]	emulation of AUG controller	no

AUG ramp-down simulations

In this work, the Fenix flight simulator has been used to simulate four discharges taken from the ITER baseline cases for AUG [2]. While their ramp-up and flattop phases are virtually identical, they differ in current ramp-down rate and in heating during the ramp-down. The aim of these shots was to develop scenarios that can terminate the discharge while maintaining good controllability. These shots are fuelled by gas puff, reaching flattop densities around $1e20m^{-3}$ at a plasma current I_p of 1.1MA. As the NBI (nominal power 6MW) and ICRH (nominal power 3MW) are applied, they go into H-mode. All shots are diverted in flattop.

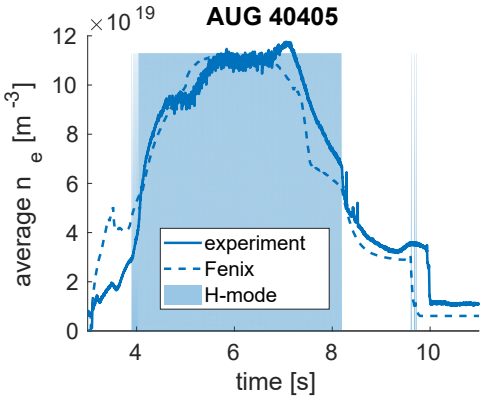

Figure 2: *Average density of AUG40405 compared to the Fenix simulation. The blue plane indicates the time in which the discharge is in H-mode.*

In order to achieve a reasonable match between Fenix simulations and the experiment, mainly two tuning knobs were used. Firstly, the parameters determining the flux of particles between the divertor, the SOL, and the walls have been manually tuned to approximate the experimentally observed average density in flattop and it's decay rate, see figure 2. Secondly, the empirical scaling coefficient of the gyro-Bohm transport coefficients in the core has been set to match the plasma energy W_{MHD} during the flattop, see middle plot of figure 3. These parameters were then kept constant for all simulations. Furthermore, the H-mode power threshold has been tuned to match the experimentally observed timing of the H-L back transition. To this end, the coefficient of the scaling law [11] which is used in Fenix by default was reduced by 10% for discharge 40405 and by 40% for 40404. With these settings applied, Fenix automatically provides a good match of the radiated power, the electron temparature T_e and the loop voltage. The shape of the separatrix corresponds well to the one obtained from equilibrium reconstruction as well.

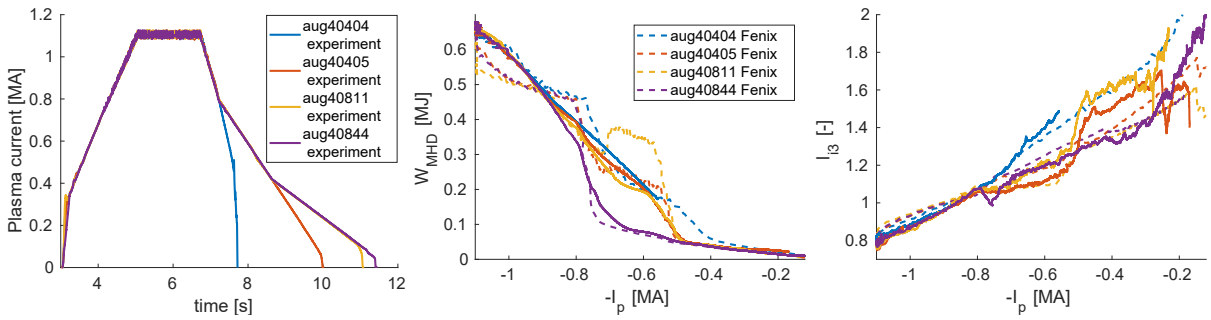

Figure 3: *I_p time traces (left) and comparison of W_{MHD} and l_{i3} to Fenix simulations plotted against I_p in the ramp down phase (middle and right) .*

l_{i3} evolution during ramp-down

Having established that Fenix manages to capture the overall trends in the discharges reasonably well, we now focus on the ramp-down phase and the self-inductance per unit length l_{i3} in particular. As l_{i3} is a measure for the peakedness of the current profile and thus for how easily the plasma can be actuated by the poloidal field coils, it is an important indicator for how difficult it is to control the plasma and the vertical instability in particular.

The bottom plot of figure 3 shows the evolution of l_{i3} during the ramp-down phase. In order to highlight the dynamics, l_{i3} is plotted against $-I_p$. The first clear trend is that l_{i3} increases as I_p is decreased. When I_p is reduced relatively fast, the current density $j_{||}$ does not have the time to equilibrate the loss of current in the plasma edge, leading to a sharper $j_{||}$ profile and thus a higher l_{i3}. By reducing the I_p ramp rate in shots 40405, 40811, and 40844, the increase of l_{i3} is reduced. This is particularly clear for the "knee point" at 0.8MA. Both trends are well captured by the Fenix simulations. The differences between 40405 and 40811 before the second knee point around 0.4MA are presumably caused by an unidentified perturbation in the experiment leading to a reduction of the confinement. As this confinement reduction did not occur in Fenix, this effect is absent and only the effect of the increased heating as a response to it is seen. Likewise, the difference between 40811 and 40844 is due to differences in the applied heating.

A third remarkable feature of discharges 40405 and 40811 is the jump in l_{i3} at the H-L transition, which is only reproduced to a very limited extent in Fenix. This jump has been studied in more detail and reproduced with the RAPTOR transport code in [3]. Figure 4 shows a comparison of l_{i3} between the experiment, Fenix, and RAPTOR. In [3], the jump in l_{i3} is explained as follows. At the H-L transition, the H-mode pedestal is lost, which leads to a strong reduction of the bootstrap current in the edge. As a result, more Ohmic current is needed in order to maintain the total I_p. Furthermore, the L-mode phase of these discharges features a very low, very flat T_e profile in the edge, leading to a high resistivity in this edge region. This causes a relatively flat current profile in the edge combined with a steep profile more inward (where T_e remains higher). Both effects lead to an increase in l_{i3}. This explanation is supported by figure 4, showing that the $j_{||}$ profile does indeed become much steeper after the H-L transition in the RAPTOR simulations, while this effect is much smaller in Fenix. This is presumably the effect of T_e not becoming low and flat enough in the plasma edge. To reproduce these effects, an improved L-mode edge model is probably required for Fenix. Adopting a two-point model

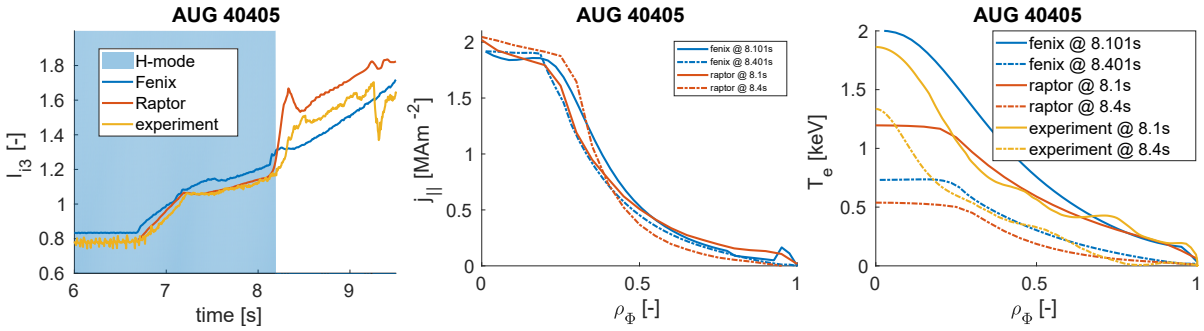

Figure 4: *Comparison of the l_{i3} jump at the H-L transition in the experiment, in Fenix and in RAPTOR [3] (left). $j_{||}$ and T_e profiles plotted against the normalised toroidal flux ρ_Φ (middle and right)* .

instead of fixed temperatures at the separatrix already provided a step in the right direction.

Conclusions and outlook

This contribution has shown that the Fenix flight simulator is capable of simulating the main features of a series of AUG discharges with varying ramp-down rates. Even though some tuning of model parameters was required and the match with experiments still is not perfect, this testifies of the capabilities of this code. The main deficiency that was uncovered in this work is that the default L-mode transport model used in Fenix cannot capture the flattening of the electron temperature in the edge. The application of Fenix to the TCV tokamak is being worked on to further investigate which of its elements are generic and which ones require tokamak-specific tuning. A comparison with TCV ITER baseline ramp-down phases [12] should allow to validate the various models. This is expected to provide indispensable insights for application of flight simulators to future machines.

Acknowledgement

This work has been carried out within the framework of the EUROfusion Consortium, partially funded by the European Union via the Euratom Research and Training Programme (Grant Agreement No 101052200 — EUROfusion). The Swiss contribution to this work has been funded by the Swiss State Secretariat for Education, Research and Innovation (SERI). Views and opinions expressed are however those of the author(s) only and do not necessarily reflect those of the European Union, the European Commission or SERI. Neither the European Union nor the European Commission nor SERI can be held responsible for them.

References

[1] E. Fable, F. Janky and W. Treutterer *et al*, Plasma Phys. Control. Fusion **64**, 044002 (2022)
[2] T. Pütterich, O. Sauter, V. Bobkov *et al*, 27th IAEA FEC (2018)
[3] S. Van Mulders *et al*, in preparation for submission to Plasma Phys. Control. Fusion
[4] E. Fable, C. Angioni, F. Casson *et al*, Plasma Phys. Control. Fusion **55**, 124028 (2013)
[5] A. Ivanov, R. Khayrutdinov, S. Medvedev *et al*, 32nd Conf. on Plasma Physics **29C**, p-5.063 (2005)
[6] M.L. Walker, G. Ambrosino, G. De Tommasi *et al*, Fusion Eng. Des. **96-97**, 716-719 (2015)
[7] M. Weiland, R. Bilato, R. Dux *et al*, Nucl. Fusion **58**, 082032 (2018)
[8] E. Poli, A. Bock and M. Lochbrunner *et al*, Comput. Phys. Commun. **225**, 36-46 (2018)
[9] S. Kim, Y. Na, S. Saarelma *et al*, Nucl. Fusion **58**, 016036 (2018)
[10] P. Stangeby, The Plasma Boundary of Magnetic Fusion Devices, IoP Publishing (2000)
[11] M. Schmidtmayr, J.W. Hughes, F. Ryter *et al*, Nucl. Fusion **58**, 056003 (2018)
[12] O. Sauter, M. Vallar, B. Labit *et al*, 28th IAEA FEC (2021)